

# Strongly-coupled anisotropic gauge theories and holography

Dimitrios Giataganas,<sup>†</sup> Umut Gürsoy<sup>‡</sup> and Juan F. Pedraza<sup>\*</sup>

<sup>†</sup>*Physics Division, National Center for Theoretical Sciences,  
National Tsing-Hua University, Hsinchu 30013, Taiwan*

<sup>‡</sup>*Institute for Theoretical Physics and Center for Extreme Matter and Emergent Phenomena,  
Utrecht University, Leuvenlaan 4, 3584 CE Utrecht, The Netherlands*

<sup>\*</sup>*Institute for Theoretical Physics, University of Amsterdam, Science Park 904,  
Postbus 94485, 1090 GL Amsterdam, The Netherlands*

We initiate a non-perturbative study of anisotropic, non-conformal and confining gauge theories that are holographically realized in gravity by generic Einstein-Axion-Dilaton systems. In the vacuum our solutions describe RG flows from a conformal field theory in the UV to generic scaling solutions in the IR with generic hyperscaling violation and dynamical exponents  $\theta$  and  $z$ . We formulate a generalization of the holographic  $c$ -theorem to the anisotropic case. At finite temperature, we discover that the anisotropic deformation reduces the confinement-deconfinement phase transition temperature suggesting a possible alternative explanation of inverse magnetic catalysis solely based on anisotropy. We also study transport and diffusion properties in anisotropic theories and observe in particular that the butterfly velocity that characterizes both diffusion and growth of chaos transverse to the anisotropic direction saturates a constant value in the IR which exceeds the bound given by the conformal value.

**1. Introduction.** Quantum many body systems in three spatial dimensions with reduced rotational symmetry have important realizations in Nature such as the quark-gluon plasma produced in non-central heavy ion collisions, or condensed matter systems described by anisotropic spin models e.g. the anisotropic 3D Ising model. The rotational symmetry in such systems can be broken by application of an external source such as an electric or magnetic field in one direction as in the various condensed matter experiments, by the geometry of the setting as in non-central heavy ion collisions, or by intrinsic properties of the interaction as in case of the anisotropic spin models or the Weyl semimetals [1].

Gauge-gravity duality [2] provides a natural avenue to study anisotropic QFTs in the presence of strong interactions. Most of the early gauge-gravity literature on anisotropic systems focuses either on scale-invariant systems or non-conformal but charged plasmas. Only the following three special cases have been studied: (i) initially conformal invariant systems where the isotropy and conformal symmetry is broken by the same mechanism, for example by a source that depends on a spatial direction as in [3–10]. (ii) Lifshitz invariant systems with isotropy as in [11]. (iii) Non-conformal charged plasmas where the anisotropy is introduced by an external magnetic field in one spatial direction as in [12–14].

In this paper we initiate a study of uncharged, non-conformal and anisotropic systems with strong interactions by means of the gauge-gravity duality. In particular, we consider a non-conformal, gapped and *confining* 4D  $SU(N)$  gauge theory in the large- $N$  limit, obtained by deforming a strongly interacting fixed point in the UV by means of a scalar operator  $\mathcal{O}$  with scaling dimension  $\Delta$ . We introduce the anisotropy by means of another operator  $\tilde{\mathcal{O}}$  that we choose to be marginal, with a coupling that depends on one of the spatial coordinates. We then study

influence of anisotropy on RG flow at zero temperature and on the thermodynamic observables and transport coefficients at finite temperature. The gauge theory is realized in holography by the Einstein-Axion-Dilaton theory in 5 dimensions with a non-trivial potential for the dilaton. This potential can be chosen such that the vacuum state confines color and there exists a phase transition at finite  $T_c$  above which a deconfined plasma state arises. This setting is similar to [3, 4], however we replace the undeformed theory that was conformally invariant in these references with a non-conformal and confining gauge theory. An especially interesting question concerns how the confinement-deconfinement phase transition in such systems are affected by the degree of anisotropy. Studying the phase diagram of the theory in case of  $\Delta = 3$  we discover that anisotropic deformation decreases the value of the confinement-deconfinement transition temperature. This is in accord with the recent lattice QCD findings [15–18] that showed both the chiral symmetry restoration and deconfinement occur at lower temperatures in the presence of an external magnetic field, a phenomenon coined “inverse magnetic catalysis”. Note that magnetic field also breaks the isotropy in a similar way as we do in our uncharged plasma. Our finding therefore brings a new twist in this story indicating that a similar phenomenon takes place even in plasmas with uncharged particles.

The vacuum state of the theory exhibits interesting behavior. In particular, in case of  $\Delta = 4$  hence  $\mathcal{O}$  marginal, the conformal symmetry in the UV is explicitly broken only by the space-dependence of the anisotropic deformation  $\tilde{\mathcal{O}}$  [19]. In this case we find a non-trivial RG flow from the conformal fixed point in the UV to a Lifshitz-like hyperscaling violating theory in the IR with a range of possible dynamical and hyperscaling violating exponents  $z$  and  $\theta$  whose values determined by the choice of

potentials in the dual gravitational theory. This freedom in the exponents  $z$  and  $\theta$  is to be contrasted with the top-down constructions from IIB supergravity [3, 4] where one obtains a Lifshitz-like IR theory with a fixed dynamical exponent  $z = 3/2$ . The models we construct here therefore opens ground for richer phenomenological applications in strongly interacting plasma physics.

After describing the holographic Einstein-Axion-Dilaton theory and presenting the background solutions in the next section, we present the scaling solutions one obtains at the end of the RG flow in section 3 and work out the thermodynamics of the corresponding plasma in section 4. Finally in section 5 we compute the anisotropic shear viscosity and the butterfly velocities as functions of temperature in these scaling solutions and provide a discussion and outlook of our findings in section 6.

**2. Holographic setup.** The gravitational theory dual to our anisotropic field theory is defined by the Einstein-Axion-Dilaton action with generic potentials  $V$  and  $Z$  for the dilaton field  $\phi$  that determine the dilaton potential energy and the coupling to the axion field  $\chi$ :

$$S = \frac{1}{2\kappa^2} \int d^5x \sqrt{-g} [R + \mathcal{L}_M], \quad (1)$$

$$\mathcal{L}_M = -\frac{1}{2}(\partial\phi)^2 + V(\phi) - \frac{1}{2}Z(\phi)(\partial\chi)^2. \quad (2)$$

Crucially, the ansatz with axion linear in one of the field theory directions,  $x_3$

$$ds^2 = e^{2A(r)} \left[ -f(r)dt^2 + d\vec{x}_\perp^2 + e^{2h(r)}dx_3^2 + \frac{dr^2}{f(r)} \right], \quad (3)$$

$$\phi = \phi(r), \quad \chi = a x_3, \quad (4)$$

automatically satisfies the equations of motion and breaks isotropy while preserving translation invariance. The solution is asymptotically AdS near the boundary  $r \rightarrow 0$  where  $A \rightarrow -\log r$ ,  $f \rightarrow 1$ ,  $h \rightarrow 0$  and  $\phi \rightarrow j r^{4-\Delta}$ . This solution generally corresponds to a non-conformal gauge theory whose IR dynamics dominated by the stress tensor  $T_{\mu\nu}$  dual to the metric and a scalar operator  $\mathcal{O} \sim \text{Tr}F^2$ , similar to the scalar glueball operator in QCD (when it is marginal), here dual to the field  $\phi$ . We call the source of this operator  $j$ . The theory is in turn deformed by a space-dependent theta term  $\tilde{\mathcal{O}} \sim \theta(x_3)\text{Tr}F \wedge F$  dual to the field  $\chi$ . The 5D Einstein-Axion-Dilaton theory can be realized in terms of D3/D7 branes in IIB string theory when  $V = 12$  and  $Z = e^{2\phi}$  [3–5]. In this case the underlying field theory is conformal. We are however interested in non-conformal, in particular *confining* gauge theories that follow from a more generic choice of the potentials  $V$  and  $Z$  [20, 21]. A choice of the form [22, 23]

$$V(\phi) = 12 \cosh(\sigma\phi) + b\phi^2, \quad Z(\phi) = e^{2\gamma\phi}, \quad (5)$$

with  $b \equiv \frac{\Delta(4-\Delta)}{2} - 6\sigma^2$ , corresponds to a gauge theory

with a scalar operator of scaling dimension  $\Delta$  that confines color in the vacuum state for  $\sigma \geq \sqrt{2/3}$  [21].

We first observe that the holographic version of the c-theorem [24] in QFT (or rather the “a-theorem” in 4D [25]) has a natural generalization in the anisotropic holographic theories. Introducing the domain-wall coordinate  $du = \exp(A(r))dr$  in (3) we find that

$$\frac{d}{du} \left\{ \left( \frac{dA}{du} + \frac{1}{3} \frac{dh}{du} \right) e^{\frac{h}{3}} \right\} < 0, \quad (6)$$

which follows directly from the Einstein’s equations for the ansatz (3). The expression inside the curly brackets is monotonically decreasing. Note that this quantity reduces to  $dA/du$  in the isotropic limit  $h \rightarrow 0$ , which is indeed the holographic analog of the a-function [24].

**3. Scaling solutions in the IR.** The RG energy scale of the dual QFT in the ground state is determined by the scale factor  $A$  of the metric (3) in gauge-gravity duality [26], which exhibits a non-trivial dependence on the holographic coordinate  $r$  when the potentials  $V$  and  $Z$  are not constant. The IR region  $r \rightarrow \infty$  corresponds to small values of  $\exp(A)$  where the dilaton grows [27] monotonically [20]. In this limit  $V \sim 6e^{\sigma\phi}$  for  $\sigma \geq 0$ . Let us focus on the case when the operator  $\mathcal{O}$  is marginal, hence  $\Delta = 4$  [28]. Here, and throughout the paper we set the source for this operator  $j = 0$  in the marginal case. We can derive the following scaling solutions in the IR limit  $r \gg 1/a$  [29],

$$ds^2 = \tilde{L}^2(ar)^{2\theta/3z} \left[ \frac{-dt^2 + d\vec{x}_\perp^2 + dr^2}{a^2r^2} + \frac{c_1}{(ar)^{2/z}} dx_3^2 \right], \quad (7)$$

$$\phi = c_2 \log(ar), \quad (8)$$

where  $\tilde{L}$ ,  $c_1$  and  $c_2$  are constants depending on  $z$  and  $\theta$ , which are given in terms of  $\gamma$  and  $\sigma$  as

$$z = \frac{4\gamma^2 - 3\sigma^2 + 2}{2\gamma(2\gamma - 3\sigma)}, \quad \theta = \frac{3\sigma}{2\gamma}. \quad (9)$$

For  $\theta = 0$  the solution exhibits a Lifshitz-like scaling

$$t \rightarrow \lambda t, \quad \vec{x}_\perp \rightarrow \lambda \vec{x}_\perp, \quad r \rightarrow \lambda r, \quad x_3 \rightarrow \lambda^{\frac{1}{z}} x_3. \quad (10)$$

For  $\theta \neq 0$ , the metric (7) has the hyperscaling violation property and transforms covariantly under (10) as

$$ds \rightarrow \lambda^{\theta/3z} ds. \quad (11)$$

When the IR theory is connected to a heat bath, one obtains the finite temperature version of the scaling metric, which is now a black-brane with blackening factor

$$f(r) = 1 - \left( \frac{r}{r_H} \right)^{3+(1-\theta)/z}, \quad (12)$$

where  $r_H$  is the location of the horizon. The black-brane

metric is obtained by multiplying the  $dt^2$  term by  $f$  and the  $dr^2$  term by  $1/f$  in (7) in the limit  $1/a \ll r \ll r_H$ . The Hawking temperature of the theory follows from requiring the absence of a conical singularity at the horizon,

$$T = \frac{|3 + (1 - \theta)/z|}{4\pi r_H}, \quad (13)$$

and transforms as  $T \rightarrow \lambda^{-1}T$  under (10). The entropy density of the plasma in the IR is obtained from the area of the horizon,

$$s = c_{\text{IR}} a^{-2 - \frac{1-\theta}{z}} T^{2 + \frac{1-\theta}{z}} / \kappa^2, \quad (14)$$

where  $c_{\text{IR}}$  is a constant. Finally, we note that the values  $z$  and  $\theta$  (and hence  $\gamma$  and  $\sigma$ ) are constrained by the bulk null energy condition as follows:

$$(z - 1)(1 + 3z - \theta) \geq 0, \quad (15)$$

$$\theta^2 + 3z(1 - \theta) - 3 \geq 0. \quad (16)$$

On top of this, the requirement of thermodynamic stability, in particular non-negativity of the specific heat  $C_V = d \log s / d \log T$ , from (14) leads to [30]

$$2 + \frac{1 - \theta}{z} \geq 0. \quad (17)$$

Combining these inequalities, we observe that for  $z \geq 1$  the value of  $\theta$  is bounded from above  $\theta \leq \theta_{\text{bound}}^{(-)}$  while for  $z \leq 0$  it is bounded from below  $\theta \geq \theta_{\text{bound}}^{(+)}$ , with [31]

$$\theta_{\text{bound}}^{(\pm)} = \frac{1}{2} \left( 3z \pm \sqrt{3} \sqrt{4 - 4z + 3z^2} \right). \quad (18)$$

The range  $0 < z < 1$  is forbidden altogether. In summary, one derives interesting universal bounds on the IR scaling behavior of strongly interacting anisotropic plasmas from holography.

**4. Thermodynamics.** One of our main motivations is to study anisotropic plasmas at finite temperature and in particular investigate the effect of anisotropy on the confinement-deconfinement transition in examples such as the QGP. Such questions pertaining thermal equilibrium can be answered by working out the free energy in the canonical ensemble, which, in the holographic description equals the Euclidean gravitational action (1) appended by the Gibbons-Hawking and counterterm actions, evaluated on-shell. We note that the counterterms in a generic Einstein-Axion-Dilaton theory were worked out in detail in [32] whose results we use but do not show here [33]. Alternatively, one can calculate the free energy directly by integrating the first law of thermodynamics  $dF = -SdT$  for  $j$  and  $a$  held fixed.

In figure 1 we plot the free energy, normalized by  $1/N^2$ , as a function of  $T$  for different choices of the anisotropy parameter  $a$  for the case of a confining gauge theory. We should divide the analysis in two cases for small  $a/j$  and

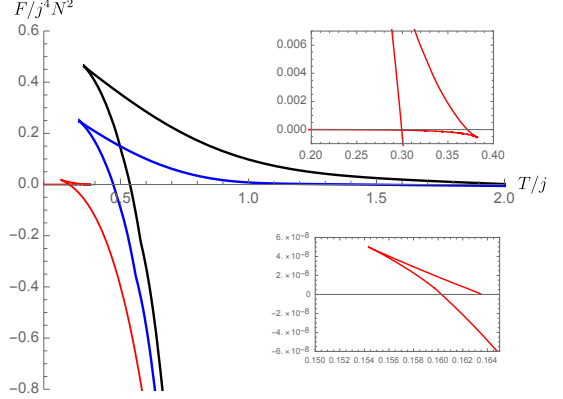


FIG. 1. Free energy as a function of  $T$  for different values of the anisotropy parameter  $a/j = 0, 1, 3$  (every dimensionful parameter is plotted in units of  $j$ ) corresponding to black (rightmost), blue (middle) and red (leftmost) curves respectively. The theory is chosen,  $\sigma = \sqrt{2/3} + 1/10$ ,  $\gamma = 1/5$ ,  $\delta = 3$  such that it yields a confining gauge theory. The horizontal axis corresponds to the confining state. All other branches corresponds to the deconfined “plasma” phases in the gauge theory. The dominant phase of the theory is given by the “lowest” branch with smallest free energy. This phase is always a plasma phase (that we call “plasma I”) at sufficiently high temperatures. As  $T$  is lowered, one encounters a single first order phase transition between this plasma phase and the confined phase, with  $F = 0$ , for smaller values  $a/j < 2.08$ . For the larger  $a/j > 2.08$ , as  $T$  is lowered, plasma I first turns into a second plasma phase (that we call “plasma II”) at a first order transition (as shown in more detail in the upper inset) and then into the confined phase through another first order transition at a lower temperature (as shown in the lower inset).

large  $a/j$  as follows. For small  $a$ , up to  $a/j \approx 2.08$  there are three competing phases at finite temperature. First, there is the *confining ground state* heated up to temperature  $T$ . The free energy of this phase is  $\mathcal{O}(1)$ , therefore it corresponds to the horizontal axis  $F = 0$  in the figure. The corresponding gravitational background is obtained from the black hole solution in (3) by sending the mass of the black-hole to zero, which in turn makes  $f = 1$ . This is the so-called thermal gas solution. Second, we observe two phases of free energy  $\mathcal{O}(N^2)$  for small  $a/j$ . These are the *deconfined, plasma phases* corresponding to the black-hole solutions (3) with a non-trivial blackening factor  $f \neq 1$ . We note that, one of these solutions, the “small black hole” (upper branches in figure 1 for the choices  $a/j = 0$  and  $1$ ) is always subdominant in the ensemble, hence can be ignored. Moreover this phase is thermodynamically unstable, with negative specific heat, as can directly be read from the figure as  $C_V \propto -d^2F/dT^2$ . On the other hand, the “big black hole” solution (lower branches in figure 1 for the choices  $a/j = 0$  and  $1$ ) dominates the ensemble for temperatures  $T > T_c$ .  $T_c$  here is given by the point the curves cross  $F = 0$ . Therefore the system is in the deconfined phase above the critical temperature  $T_c$ . This plasma phase is

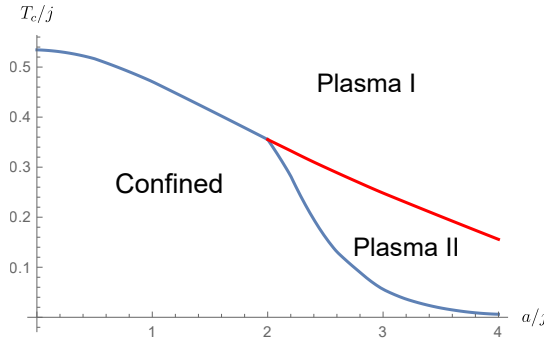


FIG. 2. Phase diagram of the system in the anisotropy parameter  $a$  and temperature  $T$ . We observe two phases, confined and ‘‘plasma I’’, for choices  $a/j < 2.08$ . For larger choices there exist three phases, confined, ‘‘plasma I’’ and ‘‘plasma II’’. The curves (both blue and red) indicate the line of first order transitions. There is a tricritical point when the dashed and the solid curves meet.

denoted as ‘‘plasma I’’ in figure 2. Below  $T_c$  the system is in the confined phase. This phase transition is of confinement/deconfinement type and it is of first order. All of this is in accordance with improved holographic QCD theory [34, 35].

For large values of  $a/j$ , specifically for  $a/j > 2.08$  the phase structure becomes more complicated. As shown in figure 1 for the choice  $a/j = 3$ , there exists now four different black hole branches with free energy  $\mathcal{O}(N^2)$  instead of aforementioned two black hole solutions, the small and the big black holes for  $a/j < 2.08$ . It is apparent from figure 1 that two of them have positive specific heat, analog of the ‘‘big black hole’’ solution in the small  $a$  case. These two solutions are denoted as ‘‘plasma I’’ and ‘‘plasma II’’ in figure 2. There are two more black hole solutions with negative specific heat, analog of the ‘‘small black hole’’ solution in the small  $a$  case. As in the small  $a$  case, these are always subdominant in the ensemble and thermodynamically unstable, hence we can safely ignore them. As shown in figure 2, there are now two phase transitions. There is the confinement/deconfinement type first order transition, analogous to the small  $a$  case, and there is a new first order transition between the two plasma phases at a higher critical temperature. Moreover, as shown in figure 2 all of these dominant phases, confined, plasma I and plasma II meet at a triple point at  $a \approx 2.08$ ,  $T/j = 0.36$ .

One essential observation is that the critical temperature  $T_c$  between the confined and the deconfined phases decrease with increasing degree of anisotropy  $a$ . This behavior is clearly shown in figure 2. This is interesting in connection to the problem of inverse magnetic catalysis [15–18]. There it is observed that the chiral symmetry breaking temperature decreases with increasing degree of anisotropy, induced by an external magnetic field  $B$ . Assuming that the chiral phase transition and the confinement/deconfinement transition share the same features—

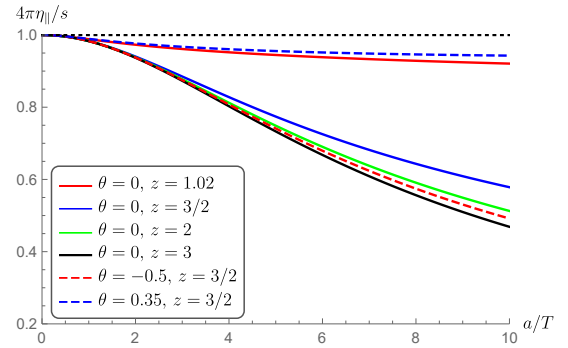


FIG. 3. The viscosity over entropy ratio for  $\Delta = 4$  and several values of  $\theta$  and  $z$ . Increase of the scaling parameter  $z$  leads to lower values of the ratio (solid lines), as well as a decrease of the value of  $\theta$  (dashed lines).

this is apparent in the lattice studies [15–18]—we find an interesting alternative explanation behind this phenomenon, that is just based on anisotropy of the medium, which in principle has nothing to do with the physics of charged particles i.e. the quarks.

**5. Transport and Diffusion.** Hadron production in heavy ion collisions is in very good agreement with a hydrodynamic description of the quark-gluon plasma and characterization of the dissipative properties plays an important role in this agreement [36]. In particular, the shear viscosity to entropy ratio in the quark-gluon plasma, and the universal value  $\eta/s = 1/4\pi$  [37, 38] that follows from the holographic calculation in the strong coupling limit, have been central in understanding these dissipative properties. It is also well understood that this universal value is violated in anisotropic systems [39–43] for the shear component parallel to the anisotropic direction,  $\eta_{\parallel}$ , whereas the shear viscosity on the plane transverse to the anisotropic direction  $\eta_{\perp}$  still attains the universal value. A calculation shows that  $\eta_{\parallel}$  can be obtained from the near-horizon form of the metric (3),

$$\frac{\eta_{\parallel}}{s} = \frac{1}{4\pi} \frac{g_{\perp\perp}}{g_{33}} \bigg|_{r=r_h} . \quad (19)$$

In figure 3 we show the behavior of this quantity for the case  $\Delta = 4$ . The curves are parametrized according to the properties of the IR geometry,  $a/T \gg 1$ , i.e. the scaling exponents  $z$  and  $\theta$ , but are valid for all values of  $a/T$ . We observe that the shear viscosity in the anisotropic direction is generally below the universal value  $\eta/s = 1/4\pi$ , which is attained in the UV. This is related to the fact that the function  $h(r)$  in (3) is positive definite for regular solutions. On the other hand, in the IR limit one obtains the following analytic expression,

$$\frac{\eta_{\parallel}}{s} = \frac{2(z-1)(1+3z-\theta)}{(4\pi)^{\frac{2}{z}-1} |1+3z-\theta|^{2-\frac{2}{z}}} \left( \frac{a}{T} \right)^{\frac{2}{z}-2} . \quad (20)$$

The power of  $a/T$  is independent of the hyperscaling violation exponent  $\theta$ . However,  $\theta$  determines the allowed range of  $z$  through (15)-(17); e.g. for the Lifshitz-like theories ( $\theta = 0$ ), the exponent is in the range  $(-2, 0]$ . More generally, the bounds imply that the power is always negative (for  $z \neq 1$ ) so  $\eta_{\parallel}$  in the deep IR takes parametrically low values approaching zero.

Another interesting dissipative phenomenon is momentum diffusion, which is related to the dissipation through shear via an Einstein relation. In holographic theories, there is a set of fundamental scales characterizing diffusion, the time scale  $\tau_L \sim 1/T$  and the “butterfly velocity”  $v_B$  [44], both entering in the diffusion constant as  $D \sim \hbar v_B^2/k_B T$ . They also happen to control the chaotic growth of the commutator  $\langle -[W(t, x), V(0, 0)] \rangle \sim \exp[(t - x/v_B)/\tau_L]$  for arbitrary hermitian operators  $W$  and  $V$ , whose properties have been studied extensively recently in [44–49]. These two seemingly unrelated concepts, chaotic behavior and diffusion can be related holographically through the near horizon dynamics where both the diffusion constant and the two scales  $\tau_L$  and  $v_B$  are calculated. Interestingly, the butterfly velocity provides a natural notion of a “light cone” even for non-relativistic systems. Very recently it was argued that  $v_B$  acts as a low-energy Lieb-Robinson velocity [48]. In anisotropic theories, there are two notions of butterfly velocities,  $v_{B\parallel}$  and  $v_{B\perp}$ , corresponding to the parallel and transverse directions, respectively [44]. These can be obtained by following how an excitation at  $\vec{x} = 0$  sent from the asymptotically AdS boundary and becomes exponentially boosted at the horizon, back-reacts on the geometry. This solution solves the Poisson equation on the curved geometry with the delta-function source  $\delta(\vec{x})$  and with an effective mass term, that corresponds to the screening length  $\mu_{\parallel}$  or  $\mu_{\perp}$  in the corresponding plasma. On the background (3) one finds,

$$\mu_{\perp}^2 = \frac{f'(3A' + h')}{2} \Big|_{r=r_h}, \quad \mu_{\parallel}^2 = \mu_{\perp}^2 e^{2h(r_h)} \quad (21)$$

and corresponding butterfly velocities  $v_B^2 = (2\pi T)^2/\mu^2$ . In the UV they both approach the conformal value  $v_B^2 = 2/3$ , while in the IR one obtains

$$v_{B\perp}^2 = \frac{1 - \theta + 3z}{2(1 - \theta + 2z)}, \quad (22)$$

$$v_{B\parallel}^2 = \frac{(4\pi)^{2 - \frac{2}{z}} (z - 1) |1 + 3z - \theta|^{\frac{2}{z}}}{1 - \theta + 2z} \left(\frac{a}{T}\right)^{\frac{2}{z} - 2}. \quad (23)$$

These expressions are to be contrasted with the butterfly velocities for isotropic theories with hyperscaling violation [44, 48]. In these works it was found that they scale generically as  $v_B^2 \sim (T_0/T)^{\frac{2}{z} - 2}$ , where  $T_0$  is a UV scale, so  $v_B^2 \rightarrow 0$  in the deep IR. In contrast, we find that  $v_{B\perp}^2$  saturates to a constant value for  $a \gg T$ . One can check, in the allowed range of  $\theta$  and  $z$  explained around equation (18), that  $v_{B\perp}^2$  and  $v_{B\parallel}^2$  are always positive definite

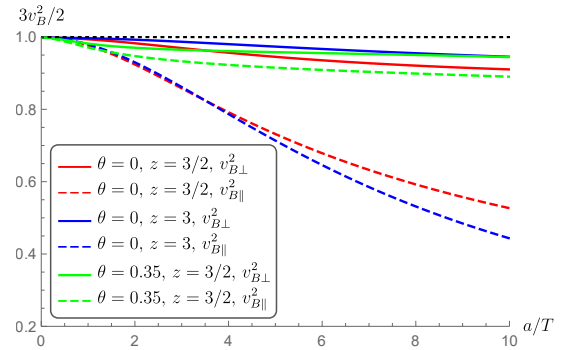


FIG. 4. The butterfly velocity in the anisotropic theory. The information diffuses slower than the isotropic theories where  $v_B^2 = 2/3$ . Notice how the increase of anisotropy slows down the growth of perturbation and that the effects are more severe along the anisotropic direction.

and smaller than 1. However, surprisingly, the value of  $v_{B\perp}^2$  in the IR can exceed the conformal value in the UV  $v_B^2 = 2/3$ . For example, for  $\theta = 0$  and  $z > 1$ , it always exceeds  $2/3$  and saturates *another bound* that is  $v_{B\perp}^2 \rightarrow 3/4$  as  $z \rightarrow \infty$ .

The results as function of  $a/T$  for intermediate values are shown in figure 4. We observe that, for sufficiently large values of  $a/T$  both velocities become smaller as one decreases  $\theta$  or increases  $z$ , while the parallel component is affected more. This is similar to the conclusion we made for  $\eta_{\parallel}/s$  above. However this behavior is reversed for smaller choices of  $a$ . We note that, even though the velocities seem to stay below the conformal value in this figure, as discussed in the previous paragraph,  $v_{B\perp}^2$  eventually exceeds this conformal value in the far IR  $a/T \gg 1$  and saturates to  $3/4$  for the choices of  $z$  and  $\theta$  in the figure.

**6. Discussion.** In this work we have uncovered several novel properties of strongly coupled anisotropic systems both in the ground state and at finite temperature. In the case of confining plasmas, we found that the confinement-deconfinement phase transition temperature decreases with the degree of anisotropy. We also discovered that this line of first order transitions ends at a second order point at a specific value of the anisotropic parameter. The fact that  $T_c(a)$  decreases with  $a$  resembles the phenomenon of inverse magnetic catalysis where both the confinement-deconfinement and the chiral phase transition temperatures decrease with the magnetic field  $B$ . The main difference is that there are no charged fermionic degrees of freedom in our case; our plasma is neutral. Given that the magnetic field also introduces anisotropy in case of the charged plasma and extrapolating our finding to that case, we suggest the possibility that the anisotropy by itself could instead be the main cause of inverse magnetic catalysis. This conjecture is to be contrasted with other proposed mechanisms, based on the fermionic contribution to the path integral [50, 51].

Quite interestingly, our proposal, the fact that anisotropy itself may be responsible for inverse magnetic catalysis can be checked by (anisotropic) lattice calculations. We also uncovered a somewhat complicated phase diagram, shown in figure 2. While, for small anisotropy  $a/j < 2.08$  there is a single first order phase transition in  $T$  between a deconfined plasma phase and a confined phase, there exists two separate plasma phases, denoted by plasma I and plasma II and a confined phase for  $a/j > 2.08$ . These three phases are connected through two first order transitions in  $T$ . It is not clear to us how to completely characterize the two separate plasma phases, apart from noting that they have different entropies. In particular it will be very important to find an order parameter for the phase transition between the two, depicted by the red curve in figure 2.

We also found that the anisotropic field theory in the ground state flows to scaling solutions in the IR, characterized by dynamical and hyperscaling violating exponents  $z$  and  $\theta$ . The theory is thermodynamically stable for a wide range of these exponents. We also obtained a generalization of the holographic c-theorem valid for the anisotropic plasmas in equation (6). It would be interesting to work out the implications of this in anisotropic field theories, and to provide a proof directly in quantum field theory.

At finite temperature the entropy of the anisotropic IR theory scales with  $T$  with exponent  $2 + (1 - \theta)/z$ . This is to be contrasted with the exponent in the isotropic case

$(3 - \theta)/z$ . Finally we studied the shear viscosity and diffusion on the anisotropy plane and found that the first can be parametrically lower than the so called universal result  $1/4\pi$  and in particular decreases with increasing  $z$  and decreasing  $\theta$ . The latter is lower than the conformal result  $v_B^2 = 2/3$  for intermediate values of anisotropy but may exceed it for larger anisotropy. This violates the bound derived and proposed in [52] and [53]. There is no contradiction however, since these papers assumed isotropy. In addition, we find that the butterfly velocity transverse to the anisotropic direction  $v_{B\perp}^2$  stays below another bound  $v_{B\perp}^2 = 3/4$  in 4 dimensions, that is attained in the limit  $z \rightarrow \infty$ . It will be interesting to figure out the field theoretic reason behind these observations. It will also be interesting to find realization of our findings in physical systems. In connection to this we refer to [54, 55] as way to measure the anisotropic shear viscosity of a strongly interacting, ultra-cold, unitary Fermi gas confined in a harmonic trap.

*Acknowledgements.*— The authors acknowledge useful conversations with Mariano Chernicoff, Chong-Sun Chu, Viktor Jahnke, David Mateos and Phil Szepietowski. This work is partially supported by the Ministry of Science and Technology of Taiwan under the grants 101-2112-M-007-021-MY3 and 104-2112-M-007 -001 -MY3, the Netherlands Organisation for Scientific Research (NWO) under the VIDI grant 680-47-518 and a VENI grant, and the Delta-Institute for Theoretical Physics ( $\Delta$ -ITP), which is funded by the Dutch Ministry of Education, Culture and Science (OCW).

- 
- [1] In this latter case isotropy is broken by separating the left and the right-handed Dirac cones along an axis in the momentum space.
- [2] J. M. Maldacena, *Adv. Theor. Math. Phys.* **2**, 231 (1998), hep-th/9711200.
- [3] T. Azeyanagi, W. Li, and T. Takayanagi, *JHEP* **0906**, 084 (2009), arXiv:0905.0688 [hep-th].
- [4] D. Mateos and D. Trancanelli, *JHEP* **1107**, 054 (2011), arXiv:1106.1637 [hep-th].
- [5] D. Mateos and D. Trancanelli, *Phys. Rev. Lett.* **107**, 101601 (2011), arXiv:1105.3472 [hep-th].
- [6] D. Giataganas, *JHEP* **1207**, 031 (2012), arXiv:1202.4436 [hep-th].
- [7] M. Chernicoff, D. Fernandez, D. Mateos, and D. Trancanelli, *JHEP* **1208**, 100 (2012), arXiv:1202.3696 [hep-th].
- [8] D. Giataganas and H. Soltanpanahi, *Phys. Rev.* **D89**, 026011 (2014), arXiv:1310.6725 [hep-th].
- [9] R. Rougemont, R. Critelli, and J. Noronha, *Phys. Rev.* **D91**, 066001 (2015), arXiv:1409.0556 [hep-th].
- [10] J. F. Fuini and L. G. Yaffe, *JHEP* **07**, 116 (2015), arXiv:1503.07148 [hep-th].
- [11] U. Gursoy, A. Jansen, W. Sybesma, and S. Vandoren, *Phys. Rev. Lett.* **117**, 051601 (2016), arXiv:1602.01375 [hep-th].
- [12] R. Rougemont, R. Critelli, and J. Noronha, *Phys. Rev.* **D93**, 045013 (2016), arXiv:1505.07894 [hep-th].
- [13] T. Drwenski, U. Gursoy, and I. Iatrakis, *JHEP* **12**, 049 (2016), arXiv:1506.01350 [hep-th].
- [14] U. Gursoy, I. Iatrakis, M. Jrvinen, and G. Nijs, *JHEP* **03**, 053 (2017), arXiv:1611.06339 [hep-th].
- [15] G. S. Bali, F. Bruckmann, G. Endrodi, Z. Fodor, S. D. Katz, S. Krieg, A. Schafer, and K. K. Szabo, *JHEP* **02**, 044 (2012), arXiv:1111.4956 [hep-lat].
- [16] G. S. Bali, F. Bruckmann, G. Endrodi, Z. Fodor, S. D. Katz, S. Krieg, A. Schafer, and K. K. Szabo, *Proceedings, 29th International Symposium on Lattice field theory (Lattice 2011): Squaw Valley, Lake Tahoe, USA, July 10-16, 2011*, PoS **LATTICE2011**, 192 (2011), arXiv:1111.5155 [hep-lat].
- [17] G. S. Bali, F. Bruckmann, G. Endrodi, Z. Fodor, S. D. Katz, and A. Schafer, *Phys. Rev.* **D86**, 071502 (2012), arXiv:1206.4205 [hep-lat].
- [18] M. D'Elia, *Lect. Notes Phys.* **871**, 181 (2013), arXiv:1209.0374 [hep-lat].
- [19] In addition there is a conformal anomaly in the theory that is incorporated in the holographic description.
- [20] U. Gursoy and E. Kiritsis, *JHEP* **02**, 032 (2008), arXiv:0707.1324 [hep-th].
- [21] U. Gursoy, E. Kiritsis, and F. Nitti, *JHEP* **02**, 019 (2008), arXiv:0707.1349 [hep-th].
- [22] S. S. Gubser and A. Nellore, *Phys. Rev.* **D78**, 086007

- (2008), arXiv:0804.0434 [hep-th].
- [23] S. S. Gubser, A. Nellore, S. S. Pufu, and F. D. Rocha, Phys. Rev. Lett. **101**, 131601 (2008), arXiv:0804.1950 [hep-th].
- [24] D. Z. Freedman, S. S. Gubser, K. Pilch, and N. P. Warner, Adv. Theor. Math. Phys. **3**, 363 (1999), arXiv:hep-th/9904017 [hep-th].
- [25] Z. Komargodski and A. Schwimmer, JHEP **12**, 099 (2011), arXiv:1107.3987 [hep-th].
- [26] A. W. Peet and J. Polchinski, Phys. Rev. **D59**, 065011 (1999), arXiv:hep-th/9809022 [hep-th].
- [27] The monotonicity is subject to a certain upper bound on  $\sigma$  [56] which we assume throughout the paper.
- [28] For relevant deformations, the system generically undergoes a confinement/deconfinement transition, so the low temperature limit is dominated by a thermal gas solution.
- [29] The form of the IR solution is independent of the choice of  $\Delta$ .
- [30] In thermodynamic systems with multiple variables thermodynamic stability is equivalent to absence of positive eigenvalues of the Hessian composed of the second derivatives of the entropy in these variables. Here the source term  $a$  indeed yields a second variable in addition to the energy. However there is no conserved charge associated to  $a$ , hence it is unclear whether this yields an additional condition.
- [31] Other observables such as correlation functions and entanglement entropy might impose further constraints on the allowed range of parameters [57]. A separate analysis would be needed for these possible additional constraints.
- [32] I. Papadimitriou, JHEP **08**, 119 (2011), arXiv:1106.4826 [hep-th].
- [33] It is worth mentioning that this counterterm action includes the conformal anomaly.
- [34] U. Gursoy, E. Kiritsis, L. Mazzanti, and F. Nitti, Phys. Rev. Lett. **101**, 181601 (2008), arXiv:0804.0899 [hep-th].
- [35] U. Gursoy, E. Kiritsis, L. Mazzanti, and F. Nitti, JHEP **05**, 033 (2009), arXiv:0812.0792 [hep-th].
- [36] J. Casalderrey-Solana, H. Liu, D. Mateos, K. Rajagopal, and U. A. Wiedemann, (2011), 10.1017/CBO9781139136747, arXiv:1101.0618 [hep-th].
- [37] G. Policastro, D. T. Son, and A. O. Starinets, Phys. Rev. Lett. **87**, 081601 (2001), arXiv:hep-th/0104066 [hep-th].
- [38] P. Kovtun, D. T. Son, and A. O. Starinets, JHEP **10**, 064 (2003), arXiv:hep-th/0309213 [hep-th].
- [39] A. Rebhan and D. Steineder, Phys. Rev. Lett. **108**, 021601 (2012), arXiv:1110.6825 [hep-th].
- [40] K. A. Mamo, JHEP **10**, 070 (2012), arXiv:1205.1797 [hep-th].
- [41] S. Jain, R. Samanta, and S. P. Trivedi, JHEP **10**, 028 (2015), arXiv:1506.01899 [hep-th].
- [42] S. Jain, N. Kundu, K. Sen, A. Sinha, and S. P. Trivedi, JHEP **01**, 005 (2015), arXiv:1406.4874 [hep-th].
- [43] J. Erdmenger, P. Kerner, and H. Zeller, Phys. Lett. **B699**, 301 (2011), arXiv:1011.5912 [hep-th].
- [44] M. Blake, Phys. Rev. Lett. **117**, 091601 (2016), arXiv:1603.08510 [hep-th].
- [45] S. A. Hartnoll, Nature Phys. **11**, 54 (2015), arXiv:1405.3651 [cond-mat.str-el].
- [46] D. A. Roberts, D. Stanford, and L. Susskind, JHEP **03**, 051 (2015), arXiv:1409.8180 [hep-th].
- [47] S. H. Shenker and D. Stanford, JHEP **05**, 132 (2015), arXiv:1412.6087 [hep-th].
- [48] D. A. Roberts and B. Swingle, Phys. Rev. Lett. **117**, 091602 (2016), arXiv:1603.09298 [hep-th].
- [49] T. Hartman, S. A. Hartnoll, and R. Mahajan, (2017), arXiv:1706.00019 [hep-th].
- [50] F. Bruckmann, G. Endrodi, and T. G. Kovacs, JHEP **04**, 112 (2013), arXiv:1303.3972 [hep-lat].
- [51] V. A. Miransky and I. A. Shovkovy, Phys. Rept. **576**, 1 (2015), arXiv:1503.00732 [hep-ph].
- [52] M. Mezei and D. Stanford, JHEP **05**, 065 (2017), arXiv:1608.05101 [hep-th].
- [53] M. Mezei, JHEP **05**, 064 (2017), arXiv:1612.00082 [hep-th].
- [54] R. Samanta, R. Sharma, and S. P. Trivedi, (2016), arXiv:1607.04799 [cond-mat.quant-gas].
- [55] R. Samanta, R. Sharma, and S. P. Trivedi, (2016), arXiv:1611.02720 [cond-mat.quant-gas].
- [56] U. Gursoy, A. Jansen, and W. van der Schee, Phys. Rev. **D94**, 061901 (2016), arXiv:1603.07724 [hep-th].
- [57] X. Dong, S. Harrison, S. Kachru, G. Torroba, and H. Wang, JHEP **1206**, 041 (2012), arXiv:1201.1905 [hep-th].